Buckling Instabilities of One-Layered Growing Tissues

Dirk Drasdo

Institut für Medizinische Informatik, Statistik und Epidemiologie, Universität Leipzig, Liebigstrasse 27, 04103 Leipzig, Germany and Max-Planck-Institut für Kolloid und Grenzflächenforschung, Theory Division, D-14424 Potsdam, Germany*

(Received 1 December 1998; revised manuscript received 22 July 1999)

Growth and folding in one-layered model tissue sheets are studied in a stochastic, lattice-free single cell model which considers the discrete cellular structure of the tissue, and in a coarse grained analytical approach. The polarity of the one-layered tissue is considered by a bending term. Cell division gives rise to a locally increasing metric. An exponential and a power-law growth regime are identified. In both regimes, folding occurs as soon as the bending contribution becomes too small to compensate the destabilizing effect of the cell proliferation. The potential biological relevance is discussed.

PACS numbers: 87.10.+e, 05.40.–a, 05.45.–a, 87.18.–h

Many growth models have been inspired by biological systems or can be applied to them, see, e.g., Refs. [1–6]. Most models consider either surface or bulk properties of more or less compact assemblies of particles (here, cells) as, e.g., in Eden-like models of tumor [2,3], bacterial [4], yeast [5], or tissue culture growth [6]. We present here a novel microscopic growth model where cell division can take place only within a single cell layer, such that a one-layered structure is maintained. In computer simulations with this model and in a coarse grained continuum approach it is shown that the growing layer cannot remain smooth but must fold by a mechanism that is believed to be generic, i.e., is independent of model details.

Such situations can occur in all biological cell systems in which cell division has to maintain a single-layered structure, e.g., in the basal (lowest) epithelium cell layer (BL) of the skin [7,8] or in crypts, the cell proliferating units in the intestine. Strong perturbations of the physiological cell division in crypts result in strong folding [8,9], producing patterns analogous to those observed during the formation of polyps or adenoma which constitute prepatterns of intestinal cancer [10].

For simplicity and in order to obtain a clear illustration of the underlying folding principle, we focus on simple one-dimensional (1D) tissue manifolds ("cell chains") in 2D space [11]. Our basic model assumptions are the existence of attractive nearest-neighbor (NN) interactions between cells to maintain the integrity of the (one-layered) tissue sheet, a bending energy that models the stabilizing effect of cell polarity on a sheet and cell division that allows potential size changes of the sheet. In order to maintain a one-cell-thick structure, cells have to be placed in the sheet again after cell division. Cells grow and divide only if this does not result in too strong cell deformations or compressions [*excluded volume* (EV) *effect*]. Hence cell division at a constant rate requires the migration of either the entire cell layer or of cells within the cell layer. Migration is assumed to be subject to strong friction. We consider situations where cells not constrained by the EV effect divide infinitely often.

We find that the growth law and geometry of the tissue sheet are determined by the competition between the destabilizing cell growth (by a proliferation of arc length) and the stabilizing bending energy of the tissue that locally confines cell movements perpendicular to the layer.

As a tissue domain grows above a certain size the bending energy becomes too small to smooth local undulations that are stochastically created by local fluctuations in the growth of arc length, and the layer roughens. If this occurs before cell deformations or compressions become so strong that cell division is hindered, the cell number increases exponentially. This is the case if the cycle time τ is sufficiently large or the bending rigidity κ is sufficiently small. Otherwise the growth law changes to subexponential growth before folding occurs.

The findings are closely related to the classical Euler buckling instability by internal strains generated by a compression of a chain or sheet [12]. In contrast, in one-layered growing tissues the strain is generated by the growth of an internally growing manifold.

Below, we first introduce the microscopic model that shows the crossover between both growth regimes as well as the folding. The instability within each growth regime is explained in an analytical approach afterwards.

The basic unit in the microscopic model is a single cell. Each cell is assumed to be spherical directly after cell division and deforms during mitosis into a dumbbell (Fig. 1a, Ref. [13]), i.e., actively changes its "equilibrium shape." To each configuration a ("total") energy is assigned according to $V^{\mathrm{tot}} = \sum_{i<j} V_{ij}^{\mathrm{NN}} + \sum_i V_i^{\mathrm{bend}} + \sum_i V_i^{\mathrm{rot}}$. V_{ij}^{NN} summarizes NN interactions that result from the competition between attractive interactions, due to adhesion molecules anchored in the cell membranes, and repulsive contributions, first from the limited cell deformability and compressibility, and second from the loss of membrane steric entropy. We choose [14]

$$V_{ij}^{\mathrm{NN}} = \begin{cases} \epsilon([\frac{2\tilde{d}_{ij}(t)}{\delta} - 1]^2 - 1) & \text{if } 0 \le \tilde{d}_{ij}(t) \le \delta\,, \\ \infty & \text{otherwise.} \end{cases} \quad (1)$$

Here, $\tilde{d}_{ij}(t) = d_{ij}(t) - 2R(t)$. For the definition of R see

 0031-9007/00/84(18)/4244(4)$15.00

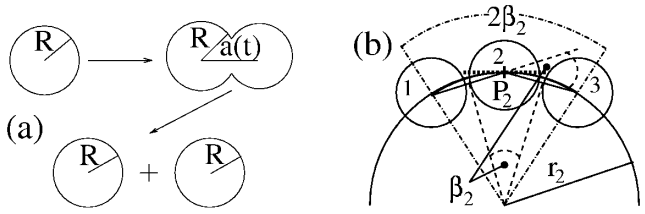

FIG. 1. (a) Cell division algorithm: During growth, a cell deforms from a spherical shape into a dumbbell by elongation of the axis from $a = 0 \rightarrow a = 2R$. (b) r_2 is the local radius of curvature for cell 2, and β_2 is its curvature angle. During deformation, cell 2 attempts to orientate its axis into the direction of the local tangent to the circle in point P_2 (dotted line).

Fig. 1. d_{ij} denotes the distance between the nearest circles of the neighboring dumbbells i and j (a circular cell is a dumbbell with axis length $a = 0$). V_{ij}^{NN} has a minimum for $\tilde{d}_{ij} = \delta/2$. The lower cutoff at $\tilde{d}_{ij} = 0$ models the EV effect. δ determines the range over which a cell can be stretched or compressed in a certain direction and is estimated to $\delta \approx 0.2R$. $\epsilon > 0$ measures the resistance against deformations. Throughout this article, $\epsilon \equiv 10$.

We introduce polarity by assuming that an anisotropic distribution of cell adhesion molecules gives rise to a bending energy V_i^{bend} in addition to V_{ij}^{NN}:

$$V_i^{\mathrm{bend}} = \frac{1}{3} \sum_{j=i-1}^{i+1} \frac{\kappa}{2} \left(\frac{1}{r_j} - c_s \right)^2 r_j \beta_j \,. \qquad (2)$$

κ is the bending rigidity, c_s is the spontaneous curvature, r_j is the local radius of curvature, and β_j is the local angle of curvature (Fig. 1b). c_s can be dropped in 1D closed geometries (see Ref. [15] and below).

To guarantee that a one-cell-thick sheet is maintained we introduce the energy contribution $V_i^{\mathrm{rot}} = \gamma(\alpha_i - \alpha_i^{\mathrm{opt}})^2$ with $\gamma \gg 1$. The angles α_i describe the momentary and α_i^{opt} describe the "optimal" orientations of the cell axis. The orientation of the axis of a nonspherical cell is assumed to be optimal if it coincides with the tangent to the local radius of curvature (Fig. 1b). This ansatz is motivated by the observation that cell division in many tissue sheets is directed, e.g., during early embryogenesis [16], in the crypt and the skin, suggesting that cells are able to detect the position of their neighbors in order to determine the direction of their division.

Active cell deformations during mitosis cause a pressure on the neighbor cells in the direction of the deformation. This leads to an increase of the total energy V^{tot}. We assume that the neighbor cells either move their center of mass or change their orientation in order to minimize V^{tot}. We further assume that (i) inertial terms are small compared to dissipative terms and (ii) processes not explicitly considered, such as the cell metabolism, intracellular movements of the cytoplasm, and the reorganization of the cytoskeleton, give rise to a stochastic component in the displacement of the cells. Although growth is intrinsically a nonequilibrium problem we have modeled the dynamics by the Metropolis method which corresponds to the numerical integration of a master equation [6,17]. This may be justified by noting that after each growth step all cells move to relax the configuration, at least into a local equilibrium [6]. In the simulations, cells are randomly chosen to perform either a small translation ($\ll R$), orientation change ($\ll \pi$), or growth ($\ll R$) trial. Each translation or rotation is accepted with probability $P_a = 1$ if $\Delta V^{\mathrm{tot}} = V_{t+\Delta t}^{\mathrm{tot}} - V_t^{\mathrm{tot}} < 0$ and with probability $P_a = \exp(-\Delta V^{\mathrm{tot}}/F_T)$ if $\Delta V^{\mathrm{tot}} \geq 0$ (hence isolated cells move diffusively in accordance with Ref. [18]). t is the time, and Δt is the time between two migration or rotation trials ($\equiv 1$ in the simulations). F_T is a "metabolic energy" [19] and the $k_B T$ analog in cellular systems (T, temperature; k_B, Boltzmann constant). It can be absorbed into a redefinition of ϵ, κ, and γ by $\epsilon \equiv \epsilon/F_T, \ldots$. A growth trial is accepted only if it does not result in too strong cell deformations, i.e., if $d_{ij} > 2R$. Between two growth trials a cell performs $n_g \gg 1$ translation and rotation trials. A cell not subject to any EV interactions has an average cycle time $\tau \propto n_g$. If EV interactions occur some growth trials are rejected and the real average cycle time becomes $\tau_R \geq \tau$. In the simulations we vary κ and τ.

In 2D space, one may distinguish between two idealized, extremal situations, a cell configuration with fixed ends at x_1, x_2 (Fig. 2a) and a closed arrangement (Figs. 2b and 2c). As $U > x_2 - x_1$ (U, arc length of the cell chain), the stretched configuration becomes curved because the minimum free energy configuration as well as the nonequilibrium configurations (Fig. 2a) become curved. As examples of curved configurations we focus in the following on closed and hence intrinsically curved cell geometries (Figs. 2b and 2c). In each simulation we start with a circular configuration of eight cells.

For small times t the circumference U and the total number of cells N grow exponentially fast, i.e., $U \propto N \propto \exp(\lambda t)$ with $\lambda = \tau^{-1} \ln(2)$ (Fig. 3a) [20]. As the time proceeds the configuration roughens and forms a regular pattern of undulations at still exponential growth if κ is small (Fig. 2c). If κ is large, first the growth law changes from an exponential to a power law $N \propto t^{1/2}$ with a cycle

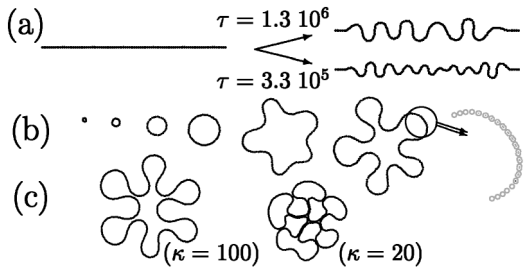

FIG. 2. (a) Buckling instability in a stretched cell configuration with fixed ends ($\kappa = 100$, left: $N = 100$, right: snapshots at $N = 110$). The larger is τ the larger are the folded domains. (b) Instability in a circular growing cell arrangement, time evolution at $N = 8$, 16, 32, 64, 128, and 256 for $\tau = 8.3 \times 10^3$ and $\kappa = 2000$ (cf. Fig. 3b). (c) Snapshots for $N = 512$, $\tau = 3.3 \times 10^6$ (cf. Fig. 3a, points A and B). The larger is κ the later folding occurs and the larger are the folded domains.

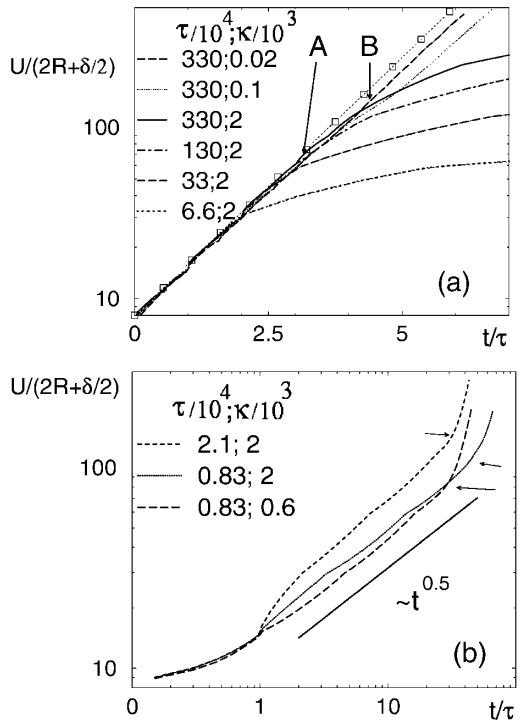

FIG. 3. Circumference U in units of $2R + \delta/2$ vs t/τ on a (a) lin-log and (b) a log-log scale. (a) The smaller κ and the larger τ the longer is the initial exponential regime (squares: $\propto 2^{t/\tau}$). At sufficiently large U a buckling instability occurs (e.g., for $\tau = 3.3 \times 10^6$ at A: $\kappa = 20$, B: $\kappa = 100$). (b) For large κ and small τ, first the growth law changes from an exponential to a power law ($\propto t^\alpha$ with $\alpha \approx 0.5$). For large t, the curve is bent upwards, indicating a buckling instability. The smaller κ and τ the smaller is the domain size at the buckling instability [A,B in (a), arrows in (b)].

time $\tau_R > \tau$. Then also in this regime a buckling instability occurs (Fig. 3b; see also Fig. 2b). The instabilities occur at typical domain sizes that grow with τ (Fig. 2a; arrows in Fig. 3b) and κ (Fig. 2c; points A and B in Fig. 3a).

The nature of the geometric instability can best be understood in a simplified continuum model. By connecting the middle points of the cells in a given configuration we arrive at a closed curve in 2D space. As in Ref. [21] we parametrize the curve by the position vector $\mathbf{r}(\alpha, t)$ where $\alpha \in [0, 1)$ is a parameter, and t is the time. $\mathbf{r}(\alpha, t)$ and its first two derivatives are periodic in α. The mechanisms which contribute to the dynamics are (a) local proliferation of arc length due to cell divisions, (b) stabilization of stretched structures by a bending energy, and (c) constant (at least on the average) circumference if cell division is switched off. We consider only cell configurations near the instability, where intersections of the curve with itself cannot occur. Then,

$$\zeta \left.\frac{\partial \mathbf{r}(\alpha, t)}{\partial t}\right|_\alpha = -\frac{1}{\sqrt{g}} \frac{\delta \mathcal{F}}{\delta \mathbf{r}} . \tag{3}$$

ζ is the friction density. $g = \partial_\alpha \mathbf{r}(\alpha, t) \partial_\alpha \mathbf{r}(\alpha, t)$ is the determinant of the metric tensor. The prefactor $1/\sqrt{g}$ ensures reparametrization invariance. $\mathcal{F} = \mathcal{F}_0(\alpha, t) - \int_0^1 \Lambda(\alpha, t) \sqrt{g}\, d\alpha$, where $\Lambda(\alpha, t)$ is a Lagrangian multiplier field which ensures that the condition for the local proliferation of length, specified below, is fulfilled. $\mathcal{F}_0 = (\kappa/2) \int_0^1 (c(\alpha, t) - c_s)^2 \sqrt{g}\, d\alpha$ is the bending energy. $c(\alpha, t)$ is the local, and c_s the spontaneous curvature. c_s can be absorbed into a redefinition of $\Lambda \equiv \Lambda - (\kappa/2) c_s^2$.

To get a closed set of equations, we have fixed a condition for the time evolution (the growth) of the local metric by

$$\partial_t \sqrt{g} = \partial_\alpha \mathbf{r} \partial_\alpha \partial_t \mathbf{r} / \sqrt{g} \equiv \sigma_k \sqrt{g}\, c^{2k} \tag{4}$$

with $k = 0, 1, \ldots$. In the exponential growth (EG) regime, $k = 0$, while in the power-law growth (PG) regime, $k = 1$. $\sigma_k > 0$ measures the strength of growth. $\sigma_0 \propto \tau^{-1}$. The choice of $k = 0$ ensures exponential growth of the metric; the choice of $k = 1$ can be shown to correspond to a normal growth velocity $G_n \propto c$ and to a transversal velocity G_t that obeys the relation $\partial_\alpha G_t = 0$. In polar coordinates, $r(\alpha, t) = r_0(t) + \xi \exp[\omega(q) t + i 2\pi q \alpha]$ and $\Lambda(\alpha, t) = \Lambda_0(t) + \eta \exp[\omega(q) t + i 2\pi q \alpha]$ ($q = 0, 1, 2, \ldots$; index "0" denotes angle-independent variables). The homogeneous equation reads $\partial_t r_0 = \sigma_k r_0^{1-2k}$, hence $r_0 \propto e^{\sigma_0 t}$ for EG and $r_0 \propto \sqrt{t}$ for PG.

To link this with the computer model, note that, for EG, cells can freely divide, hence $N \propto \exp(\lambda t) \propto U = \int_0^1 \sqrt{g}\, d\alpha$. For homogeneous growth, $U = 2\pi r_0$. If, as for PG, a cell is jammed between its right and left neighbors it can grow only if it previously had moved such that free space for its next growth step is provided, i.e., if it moved into the angle interval $\beta \propto c$ (for $\beta \ll \pi$) (see β_2 for cell 2 in Fig. 1b). Hence in a homogeneous configuration an increase of r_0 occurs according to $[r_0(t + \Delta t) - r_0(t)]/\Delta t \propto \beta \propto 1/r_0$ ($r_0 \gg R$), resulting in the observed growth law.

A linear stability analysis in the coarse grained approach around the homogeneous growing circle (where r determines the dynamics of Λ) yields

$$\omega(q) = -\frac{A q^2 (q^2 - 1)^2}{q^2 + 1} + \frac{B (q^2 - 1)(q^2 - 1 + 2k)}{q^2 + 1} \tag{5}$$

with $A = \kappa/(r_0^4 \zeta)$, $B = \sigma_k / r_0^{2k}$. For $q^2 \gg \max(1, 2k - 1)$, $\omega(q) \approx -Aq^4 + Bq^2$ as, e.g., for particular cases of dendritic [22] and molecular beam epitaxial growth [23]. If no growth occurs ($\sigma_k = 0$) the circle is the only stable solution. Otherwise, $\omega(q = 0) = \sigma_0 > 0$ for EG, so homogeneous deviations grow. For PG, $\omega(0) = -\sigma_1 / r_0^2$, so homogeneous perturbations are damped out. $\omega(q = 1) = 0$, i.e., a translation of the circle is marginally stable [15]. ω has a second zero at $q_c^2 = X$ for $k = 0$ and $q_c^2 = [1 + X + \{(1 - X)^2 + 8Xk\}^{0.5}]/2$ for $k > 0$, with $X \equiv B/A = \zeta \sigma_k r_0^{4-2k}/\kappa$. For $1 < q < q_c$, $\omega(q) > 0$. For $q \to \infty$, $\omega(q) < 0$; i.e., short wavelength perturbations are damped out. The fastest growing mode is $q_m^2 \approx X/2$ (if $q_m \gg 1$). q_c and q_m grow with increasing X. The buckling instability occurs at domain sizes $\propto q_c^{-1}$ which decrease with increasing growth strength and decreasing

bending rigidity, in agreement with the tendencies found in the computer simulations. At the instability the bending energy does not suffice anymore to smooth the roughening effect of the cell proliferation. A decrease of the cycle time has the same effect: the "time" between two subsequent cell divisions does not suffice anymore to smooth local undulations. For PG, cells at positions with larger than average local curvature have a smaller than average mitotic cycle, and thus divide faster than cells at positions with smaller local curvatures. This further increases the difference in the local curvatures in a self-enhancing process resulting in a folding of the domain. For EG, the increment in the metric is proportional to the metric already proliferated.

The folded structures are not in equilibrium: for the 1D ring structures, the undulations regress if the cell division is suppressed. There is no contribution due to shear. Also 2D buds formed in 3D may reorganize into a perfectly smooth layer on large time scales and reduce shear energy. This line of argument is supported by observations which show that cell assemblies can behave as viscoelastic fluids: under compression between two plates, cell assemblies first deform followed by a reorganization of the cells in order to reduce elastic energy contributions [24]. A separate experiment identified cells to diffuse even within cell aggregates [18]. However, growth in a 2D surface for some cases is expected to be at least temporarily accompanied by shear stress that elevates the energy barrier for the instability, but is not expected to change its nature.

This folding mechanism may be present in all one-layered epithelial tissues including those embedded in soft connective tissue during development or the maintenance of tissue if the cycle time or the tissue bending stiffness become sufficiently small (the latter, e.g., by weakening the cytoskeleton) either by internal or external stimuli. An example may be the postirradiational situation in crypts [8,9]. Crypts form pear-shaped pockets in the intestinal wall [25]. They are responsible for the maintenance of the high cell turnover in the intestine. After x-ray irradiation the cell proliferation stops for a short time followed by a period of very rapid cell division. This leads to an increase of the crypt size and fingerlike instabilities in the floors or walls of the crypts, indicating that the cell migration is no longer able to balance the cell division. Folding can also be observed in other geometries. After administration of the growth factor, the cell proliferation increases in the skin of the mouth accompanied by a thickening of the skin and stronger undulations of the BL (where most divisions occur) [7,8]. The (extra) buckling may indicate that the increased cell proliferation is no longer balanced by the cell migration out of the BL; the thickening that the cell loss into the oral cavity is too slow.

As shown in [26] for blastula formation, all simulation parameters can be related to experimental quantities.

D. D. thanks M. Loeffler much for discussions and the hint to Refs. [9,10], and thanks G. Forgacs, M. Kschischo, C. S. Potten, U. Seifert, and especially G. Gompper for discussions or suggestions pertaining to the manuscript. This work was supported by the Deutsche Forschungsgemeinschaft under Grant No. LO 342/4-3.

*Present address.

[1] J. Krug and D. Spohn, in *Solids Far From Equilibrium*, edited by C. Godreche (Cambridge University Press, New York, 1991).
[2] M. Eden, in *Proceedings of the 4th Berkeley Symposium on Mathematics and Probability*, edited by J. Neyman (University of California Press, Berkeley, 1961), Vol. IV.
[3] A. Bru *et al.*, Phys. Rev. Lett. **81**, 4008 (1998).
[4] E. Ben-Jacob *et al.*, Phys. Rev. Lett. **75**, 2899 (1995).
[5] T. Sams *et al.*, Phys. Rev. Lett. **79**, 313 (1997); J. M. Lopez and H. J. Jensen, Phys. Rev. Lett. **81**, 1734 (1998).
[6] D. Drasdo *et al.*, Phys. Rev. E **52**, 6635 (1995).
[7] C. L. Farrell *et al.*, Int. J. Radiat. Biol. **75**, 609 (1999); see Fig. 3, and private communications.
[8] C. S. Potten *et al.* (to be published); (private communication).
[9] A. B. Cairnie and B. H. Millen, Cell Tissue Kinet. **8**, 89 (1975).
[10] K. Araki *et al.*, Gastroenterology **109**, 1468 (1995).
[11] An appropriate starting point for a 3D generalization is Eqs. (3) and (4), together with the physics described, e.g., in W. Cai *et al.*, J. Phys II (France) **4**, 931 (1994) (for fluid membranes in $d = 3$); also in M. Marsili *et al.*, Rev. Mod. Phys. **68**, 963 (1996) (for arbitrary d).
[12] L. Golubović *et al.*, Phys. Rev. Lett. **81**, 3387 (1998); D. Moldovan and L. Golubović, Phys. Rev. Lett. **82**, 2884 (1999).
[13] Some simulations use the slightly different division algorithm of Ref. [6] which produces equivalent results.
[14] The results are insensitive to the exact shape of V_{ij}^{NN}.
[15] U. Seifert, Phys. Rev. A **43**, 6803 (1991).
[16] J. G. White and G. G. Borisy, J. Theor. Biol. **101**, 289 (1983).
[17] N. Metropolis *et al.*, J. Chem. Phys. **21**, 1087 (1953); F. Graner and J. A. Glazier, Phys. Rev. Lett. **69**, 2013 (1992); G. Gompper and D. M. Kroll, Phys. Rev. E **52**, 4198 (1995).
[18] J. C. M. Mombach and J. A. Glazier, Phys. Rev. Lett. **76**, 3032 (1996).
[19] D. Beysens *et al.*, in *Dynamical Networks in Physics and Biology*, edited by D. Beysens and G. Forgacs (Springer, New York, 1998).
[20] This growth law is precisely observed during blastula formation, where, e.g., in *synapta digita* or *sea urchin*, a hollow sphere is formed from the oocyte by successive cell divisions [cf. S. F. Gilbert, *Developmental Biology* (Sinauer, Sunderland, MA, 1991), 3rd ed.]; see also Ref. [26].
[21] R. E. Goldstein and S. A. Langer, Phys. Rev. Lett. **75**, 1094 (1995).
[22] D. A. Kessler *et al.*, Adv. Phys. **37**, 255 (1988).
[23] A. Pimpinelli and J. Villain, *Physics of Crystal Growth* (Cambridge University Press, Cambridge, England, 1998).
[24] G. Forgacs *et al.*, Biophys. J. **74**, 2227 (1998).
[25] C. S. Potten and M. Loeffler, Development **110**, 1001 (1990).
[26] D. Drasdo and G. Forgacs, Dev. Dyn. (to be published).